International Journal of Multiphysics
Volume 18, No. 4, 2024
ISSN: 1750-9548

Thermodynamic Modeling of a Hybrid Desalination System Using Solar Energy and Solid Wastewater Technology

Pouria Morad Alizadeh[1], Taleb Zarei[2], Ehsan Abedini[3], Jamshid khorshidi Mal Ahmadi[4]

[1].Corresponding author, doctoral student In mechanics, Hormozgan University
[2] . Associate Professor of Chemical Engineering, Hormozgan University, Bandar Abbas
[3] . Associate Professor of Mechanical Engineering, Hormozgan University, Bandar Abbas
[4] . Associate Professor of Chemical Engineering, Hormozgan University, Bandar Abbas

Abstract

Solar energy has been used for various purposes in human societies for a long. Over the last few decades, the intensification of global warming has led to an increase in demand for new technologies to produce renewable energy without toxic by-products for the environment and climate dynamics of the planet. In this field, concentrating solar collectors play an outstanding role because they can absorb solar energy and convert it into thermal, mechanical, or electrical power, without producing excess waste. In this study, a concentrating solar collector with a parabolic-trough geometry was designed using a collector tube consisting of two concentric glass tubes with a vacuum in the annular space using water as the absorber fluid. To improve thermal utilization, a copper probe was embedded inside the tube to separate the flow of cold and hot water. The inlet fluid temperature and mass flow rate were assumed equal to 25°C and 0.08 kg/s, respectively. The wind speed in the first part of the analysis was considered 5 m/s. The support bracket connected to the solar absorber is the main source of heat loss inside the system due to exposure to the ambient air. Such heat losses negatively affect the absorber outlet temperature, which in turn reduces the efficiency of the system. The heating of the absorber leads to an increase in the amount of heat transferred to the fluid. The resulting heat is lost due to radiation through the glass cover and conveying it to the support bracket. The temperature gradient is affected by different wind speeds. This is because more than 98% of the surface of the support bracket is exposed to the ambient air, which is the main source of heat loss. Increasing the number of support brackets connected to the absorber tube causes an increase in heat loss. In addition, the thermophysical properties of the support bracket material, such as thermal conductivity and its capacity to store heat affect the heat exchange.

Keywords: PTSC, solar energy, inlet fluid flow, inlet fluid temperature, thermal losses

Introduction

The negative consequences of global climate change and the report of experts on the catastrophic future have led the minds and measures to search for a sustainable energy policy. With a low rate of greenhouse gas emissions, Iran is one of the most vulnerable countries in the Middle East, which has initiated many mitigation policies and measures to exploit low-carbon energy sources in recent years [1]. PTSC is one of the solar energy exploitation systems with more advantages such as co-production, better efficiency, and the possibility of high thermal storage compared to photovoltaic systems. Unlike photovoltaic systems, the conversion of solar energy into electricity in PTSC is indirect. Like other concentrating solar technologies, its central function is to collect solar rays, concentrate them on the solar absorber, and transfer them to HTF in the form of useful heat. As shown in Fernandez-Garcıa et al., PTSC has various applications [10][11]. Due to the complexity of the PTSC system, several scientific studies in this field have provided different solutions for modeling, numerical simulation, testing, and identification of economic and techno-economic aspects [12], [13], [14],[15]. Based on the same

operating principle, PTSCs offer different designs and alternative proposals depending on the context [16]. Also, to improve optical and thermal efficiency, they reduce the costs of building and developing more compact designs. When the collector concentrates the solar rays on the surface of the absorber tube, the heat flux distribution is non-uniform and affects the optical efficiency [17], [18]. In most of the studies, presuppositions based on flux uniformity have been proposed to simplify the study. Several techniques have been proposed to analyze concentrated flow density and optical efficiency based on ray tracing, such as the Monte Carlo method [19][20]. Additionally, photogrammetric techniques have been used to evaluate non-uniform flows and optical analysis. Also, studies have been conducted in the field of PTSC thermal analysis focusing on heat exchanges [21], [22], [23]. Several methods have been proposed regarding the use and selection of HTFs to improve the thermal efficiency of the system [24], [25], [26], and other aspects in the research literature [14]. Considering the climatic characteristics of PTSC deployment areas, some studies have proposed mathematical models simulated under several approaches. For example, researchers in [27] investigated the simulation and performance analysis of a one-dimensional PTSC model with two fluids in the Algerian desert. Marefati et al. [28] used PTSC to evaluate the potential of solar energy in four Iranian cities and considered its performance in different meteorological conditions with several input parameters and discussed the results. Babikir et al. [29] proposed a single-dimensional thermal model of PTSC in a quasi-steady state and tested four HTFs (treated water, untreated water, Therminol VP-1, and Therminol 66) to perform a comparative thermal analysis of behavior and application in coastal climatic conditions. However, in the model [29], some aspects affecting the performance of the system are considered insignificant. The limitations of the model proposed in [29, 30] are the fundamental principles of the current work as follows. First, it does not reach the ends of the heat collecting element (HCE) or solar receiver as the solar radiation angle increases from zero. Such non-illuminated parts of the HCE affect the optical efficiency of the system. Secondly, the HCE is connected to the concentrator through metal supports called fins. The number of supports varies according to the PTSC prototypes produced. In most cases, there are at least two support brackets. The cross-section in contact with the HCE recovers part of the heat. The heat recovered by natural convection or forced convection is dispersed and increases the heat loss of the system. The research literature shows that the former case is not considered in mathematical modeling and numerical simulation of the PTSC system, such as Padilla et al. [22]. This is because the researchers assumed that there was no loss in their system. Marif et al [27] did not include this aspect in their study. This overestimates the input heat flux in the HCE. However, some works have also considered this aspect, such as Marefati et al. [28]. Alfellag [36] used the approach proposed by Lippke [40] to calculate the final losses. Also, Behar et al. [37] calculated the final losses with Gaul and Rabe's relation [38, 41]. Their selection shows that this approach brings reasonable results. In none of the studies, this aspect was combined with an hourly solar radiation estimation model or a solar tracking system to complement the optical model. In addition, overall system performance evaluation is not done daily. A correct representation of such a prominent thermal phenomenon during the normal hourly operation of the PTSC system on a given day is not provided. The second case has been discussed in the research literature. For example, focusing on heat transfer analysis and modeling of the parabolic-trough solar receiver (implemented in Engineering Equation Solver (EES) software), Forristall [21, 41] modeled the support bracket. The researcher has introduced the support bracket as a source of heat loss in the system but has not analyzed its thermal effects on the performance of the system in detail. In his work, Padilla [23] has modeled the support bracket considering fins. The results show that the used model is thermally better and more conservative than the model [21, 42]. Similarly, Liang et al. [31] and Behar et al. [37] incorporated different approaches for thermal modeling of the support bracket in their HCE thermal models. However, their thermal effects have not been analyzed. In most studies, support brackets thermal models have been selected without an optimal selection criterion. This can be considered a limitation in the thermal performance analysis of PTSC systems. Although this simplifies the analysis assumptions, it underestimates the radiation losses at the outer surface of the HCE, the losses through the support brackets as well as the exit fluid. This study aims to propose a mathematical model for PTSC based on the coupling of optical and thermal models, taking into account the aspects mentioned above (as one of the limitations of the model in [29, 43]) and the usability in climate conditions of south and southeast Iran. Also, an optical model of PTSC considering the final loss of HCE is proposed, along with a solar radiation estimation model based on a single-axis solar tracking system.

Physical model

The PTSC (Figure 1a) is assembled on a metal structure placed on the ground. The collector consists of a set of mirrors with high reflectivity to reflect the maximum solar flux collected on the solar receiver. The solar receiver consists of a transparent glass cover with a high absorption coefficient, low emission, and high transmission. The glass cover covers the absorber tube containing the HTF. The solar receiver is located linearly at the focus of the collector at a distance *f*. It is also attached to the collector through the support brackets as shown in the figure. Figure 1b shows the regions near the end of the HCE that are not illuminated by solar radiation reflected from the collector. When the PTSC lacks a full two-axis tracking system and the incidence angle increases (different from zero), the entire surface of the HCE cannot be illuminated. This means that the system cannot receive the radiation collected by the sun reflector. This usually affects the end of the HCE. These losses are generally referred to as end losses (Xend). Due to the lack of use of the two-axis tracking system, these losses are not considered in this study. The technical specifications and dimensions of the physical model are borrowed from [29].

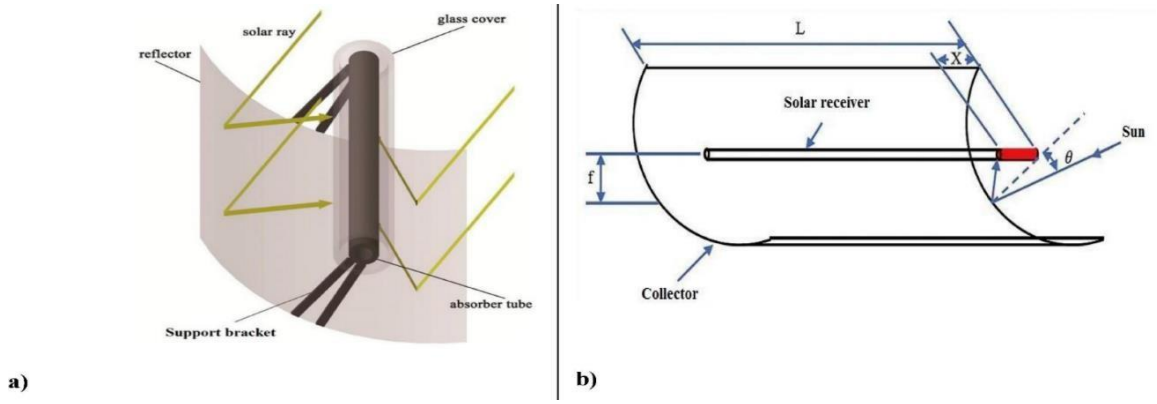

Figure 1: a) schematic of a PTSC [31] b) ending HCE losses [28]

Equations governing parabolic-trough collector (PTC):

Parabolic-trough collector is used in this study due to high heat transfer with low cross-sectional area, relatively simpler technology than other methods, and temperature increase up to 400 degrees Celsius.

The geometrical analysis of the parabolic-trough collector is discussed below.

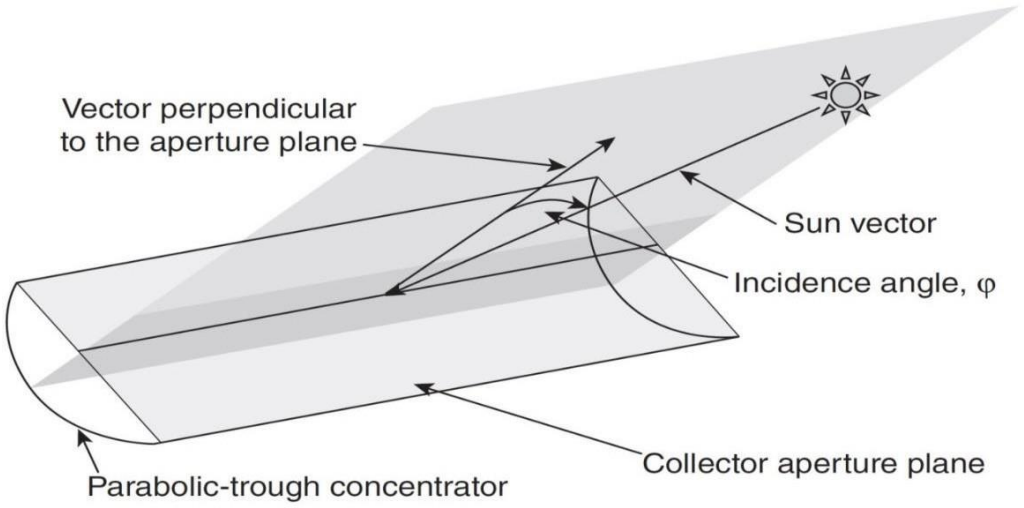

Figure 2: Correct deployment position of parabolic-trough collector

Figure 2 represents the important computational parameters.

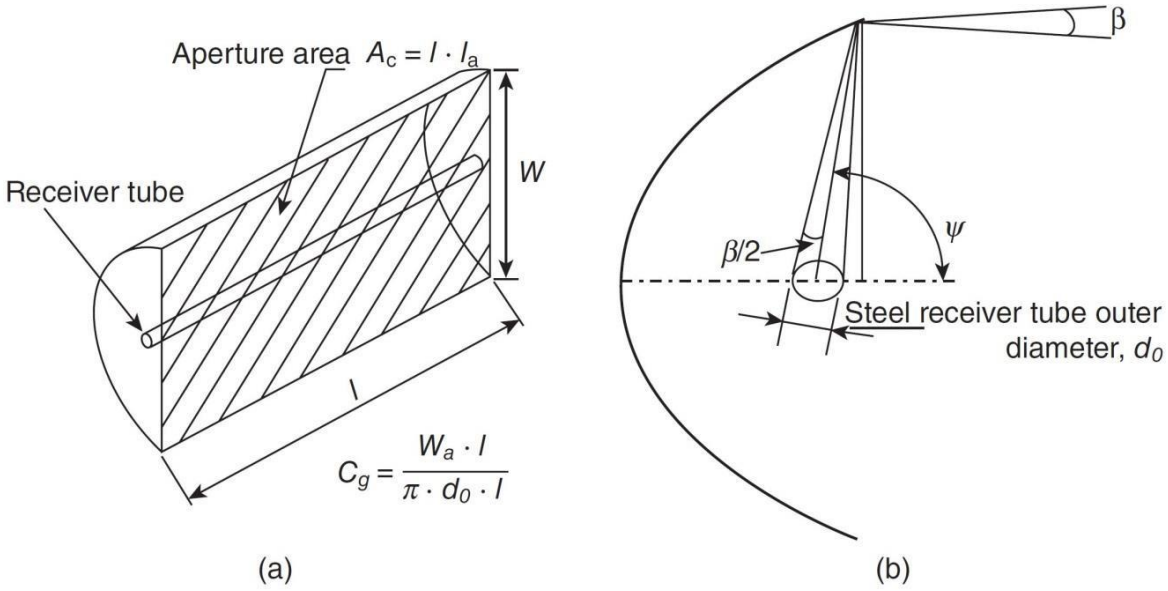

Figure 3: a) geometric concentration ratio C_g b) acceptance angle β and aperture angle Ψ of parabolic-trough collector

$$C_g = \frac{W.l}{\pi.d_o.l} = \frac{W}{\pi.d_o} \quad 1\text{-}6$$

where W is the width of the collector aperture, l is the length of the collector, and d_o reflects the outer diameter of the absorber tube.

One of the important parameters of the parabolic-trough collector is $\eta_{opt,0^\circ}$, which indicates the optical efficiency and is obtained as the product of 4 parameters, i.e. reflection, blocking factor, coefficient of passing through the glass of the absorber tube, and absorption coefficient of the absorber tube.

$$\eta_{opt,0^\circ} = \rho \times \gamma \times \tau \times \alpha_{\varphi=0^\circ} \quad 2\text{-}6$$

Optical efficiency between 0.74 and 0.79 is considered desirable and high quality for parabolic-trough collectors.

The value of $\eta_{opt,0^\circ}$ is the maximum efficiency and changes according to the change of the angle of incidence (φ). As a result, a correction factor is needed as the angle of incidence correction factor ($k(\varphi)$). This correction factor is calculated using a polynomial as represented in Equation 3.

$$k(\varphi) = 1 - 2.23073 * 10^{-4} * \varphi - 1.1 * 10^{-4} * \varphi^2 + \quad 3\text{-}6$$
$$\begin{cases} 3.1896 * 10^{-6} * \varphi^3 - 4.85509 * 10^{-8} * \varphi^4 & 0^\circ < \varphi < 80^\circ \\ k(\varphi) = 0 & 85^\circ < \varphi < 90^\circ \end{cases}$$

Based on the correction factor, the optical efficiency is calculated according to Equation 4-6.

$$\eta_{opt,\varphi\neq0^\circ} = \eta_{opt,0^\circ} k(\varphi) \quad 4\text{-}6$$

In order to calculate the energy transferred from the collector to the working fluid inside the absorber, the law of conservation of energy is applied to the system.

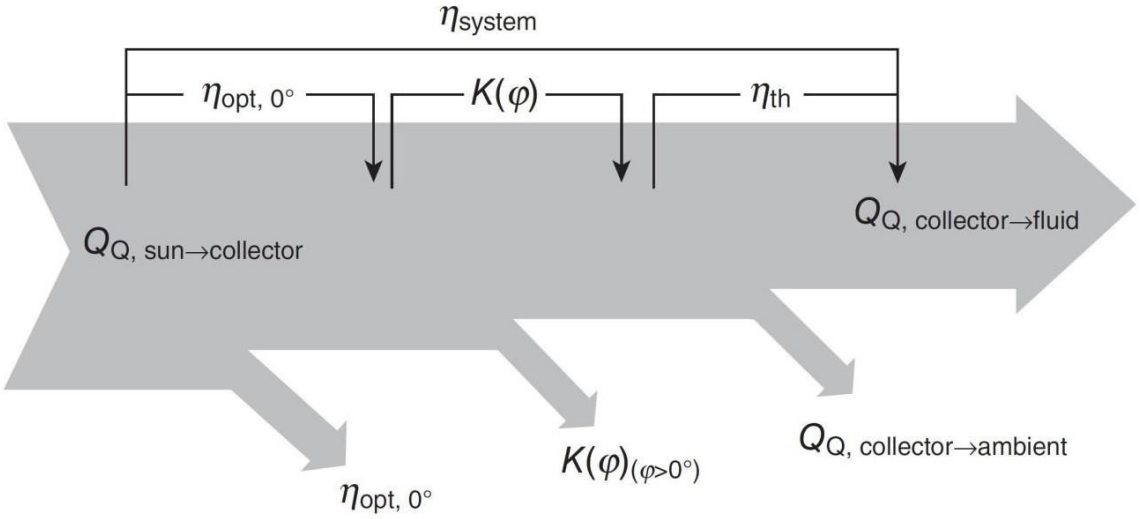

Figure 4: Energy conservation in parabolic-trough collector

$$\eta_{system} = \frac{Q_{Q,collector \rightarrow fluid}}{Q_{Q,sun \rightarrow collector}} \quad 6\text{-}6$$

$$Q_{sun\_collector} = A_c . E_d . \cos(\varphi) \quad 6\text{-}7$$

$$Q_{collector\_fluid} = \dot{m} . (h_{out} - h_{in}) \quad 6\text{-}8$$

where A_c is the opening area and E_d shows the direct solar radiation.

Applying the energy balance to Equation 6-9 leads to the following figure.

$$Q_{collector\_fluid} = A_c . E_d . \cos(\varphi) . \eta_{opt,0^\circ} k(\varphi) . F_e - Q_{collector\_ambient} \quad 6\text{-}9$$

where F_e is the coefficient of soil contamination of the collector and its value in commercial collectors varies between 0.95 and 1.

Thermal model

The developed thermal model is a one-dimensional model in which the support brackets connecting the collector to the absorber tube are modeled. Also, the heat exchanges of the system (Figure 5) are analyzed. The multiplicity of models to quantify heat flow through support brackets and its effect on thermal performance directs our attention to five thermal models.

In the first model known as Model 0, the support bracket is ignored and not modeled. In the second model, known as Model 1, the bracket thermal model developed by Forristall [21] is used. In the third model, called Model 2, the support bracket thermal model developed by Padilla et al. [22] is considered. In the fourth model, called Model 3, the approach used by Liang et al. [31] is used to model the support bracket. In the fifth model, called Model 4, the approach of Behar et al. [37] is used. These five thermal models are coupled with optical models and solar radiation estimation models for thermal simulation and analysis. The details of the thermal analysis are as follows.

$$A_e K_e \left(\frac{\partial^2 T_e}{\partial X^2}\right) + \eta_{opt} I_{Beam} A_{col} - [\pi D_{e,ou} h_{e-a,conv,ou}(T_e - T_a) + \pi D_{e,ou} h_{e-a,rad,ou}(T_e - T_s)] + [\pi D_{ab,ou} h_{ab-e,conv,ou}(T_{ab} - T_e) + \pi D_{ab,ou} h_{ab-e,rad,ou}(T_{ab} - T_e)] = 0$$

$$A_{ab}K_{ab}\left(\frac{\partial^2 T_{ab}}{\partial X^2}\right) + \eta_{opt}Q_{col}A_{ab} - [\pi D_{ab,ou}h_{ab-e,conv,ou}(T_{ab} - T_e) + \pi D_{ab,ou}h_{ab-e,rad,ou}(T_{ab} - T_e)] + [\pi D_{ab,in}h_{ab-f,conv,in}(T_{ab} - T_f) + h_{b,cond}(T_b - T_a)] = 0$$

$$A_f K_f\left(\frac{\partial^2 T_f}{\partial X^2}\right) - \dot{m}_f C_{p,f}\frac{\partial T_f}{\partial x} + \pi D_{ab,in}h_{ab-f,conv,in}(T_{ab} - T_f) = 0$$

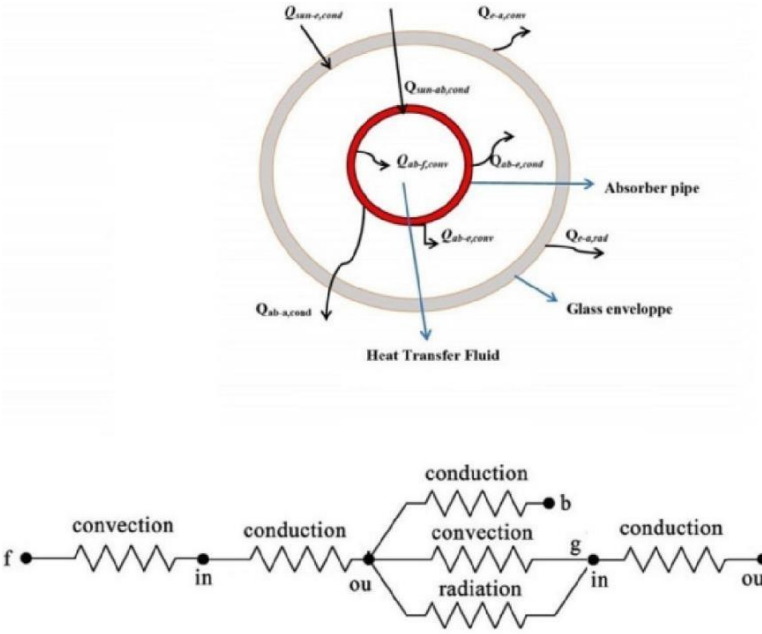

Figure 5: Schematic of heat exchange process in PTSC and thermal resistance pattern [37]

Results and discussion

PTSC is simulated with different aspects considered in mathematical modeling. The input parameters of the receiver are represented in Table 1. The simulation process was carried out in MATLAB with a wind speed equal to 5 m/s and data for a period of 5 months from Southeastern Iran Electricity Company. Thermal functions are quite sensitive to changes in input values.

Table 1: Input parameters of the proposed PTSC

Parameters	Unit	Value
The inner diameter of the absorber	*m*	0.0158
The outer diameter of the absorber	*m*	0.0178
The inner diameter of the glass cover	*m*	0.057
The outer diameter of the glass cover	*m*	0.06
The length of the collector	*m*	3.4
The width of the collector	-	1.1
Tracking factor	-	0.48
Glass cover transfer	-	0.9

Absorption coefficient of the absorber	-	0.9
Absorption coefficient of glass cover	-	0.02
Stefan–Boltzmann constant	-	5.67*10^-8

The thermal performance is measured based on the HTF outlet temperature as a comparative variable in the validation. Therefore, various experiments were performed by changing the input parameters of the model such as radiation, fluid mass flow rate, and fluid inlet temperature to obtain different fluid outlet temperatures. As shown in Figure 6, HTF fluid velocity, HTF convection heat transfer coefficient, and total heat loss from the glass to the environment relative to the HTF flow rate were analyzed (5-1). According to the drawn plots, increasing the flow rate of HTF causes a slight increase in the total heat loss. At the same time, increasing the flow rate of HTF causes rapid enhancement of the heat transfer coefficient and fluid speed of HTF.

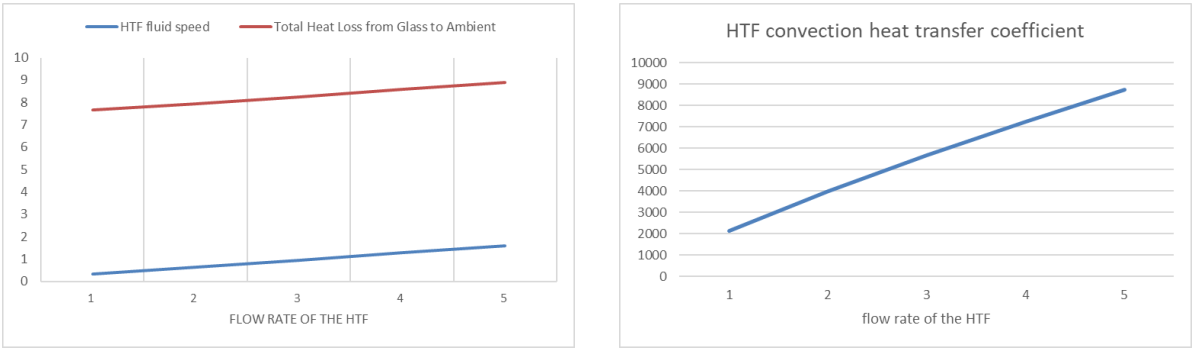

Figure 6: a) HTF fluid speed changes, and total heat loss from glass to the environment relative to the HTF flow rate b) HTF convection heat transfer coefficient in relative to HTF flow rate

Considering the HTF flow rate equal to 1 and variable inlet temperature (25.3 - 65.3), values of HTF convection heat transfer coefficient and total heat loss from glass to the environment are analyzed. According to Figure 7, increasing the inlet temperature increases the convection heat transfer coefficient. Up to a temperature of less than 35.3 degrees, the total heat loss is very low. From the temperature of 35 to 45, a very large increase (83.92%) in the total heat loss is achieved and the upward trend continues.

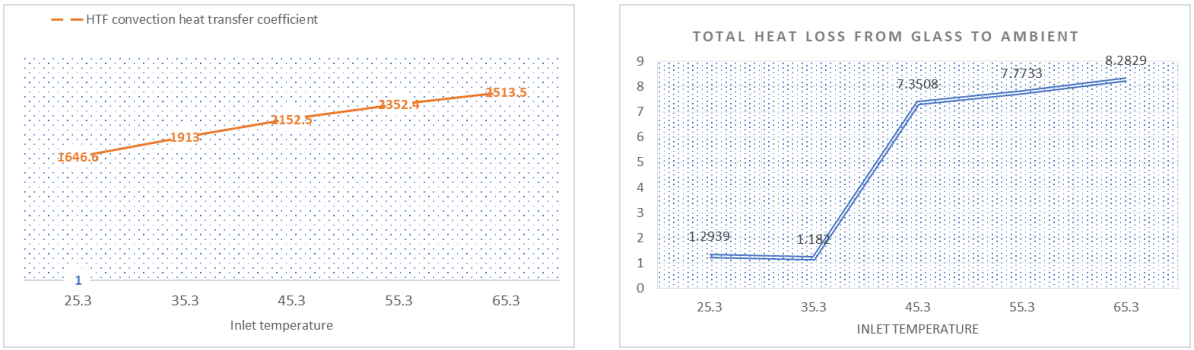

Figure 7: a) Variations of HTF convection heat transfer coefficient and total heat loss from the glass to the environment relative to the inlet temperature

According to the results of the experiments, when the fluid inlet temperature to the HCE is not too high (about 100°C) under constant solar flux (about 930 W/m2), the fluid heats up at a significant rate.

The inlet fluid temperature and mass flow rate were assumed equal to 25°C and 0.08 kg/s, respectively. The wind speed in the first part of the analysis was considered to be 5 m/s. The support bracket connected to the

solar absorber is the main source of heat loss inside the system due to exposure to the ambient air. Such heat losses negatively affect the absorber outlet temperature, which in turn reduces the efficiency of the system. Figure 8 shows the daily changes in the solar absorber output temperature. An increase in solar radiation leads to an increase in losses. The heating of the absorber leads to an increase in the amount of heat transferred to the fluid. The resulting heat is lost due to radiation through the glass cover and conveying it to the support bracket. The temperature gradient is affected by different wind speeds. This is because more than 98% of the surface of the support bracket is exposed to the ambient air, which in turn is the main source of heat loss. Increasing the number of support brackets connected to the absorber tube causes an increase in heat loss. In addition, the thermophysical properties of the support bracket material, such as thermal conductivity and its capacity to store heat affect the heat exchange. The output temperature of the absorber of the proposed model is strongly correlated with different amounts of solar radiation during the day. This may be caused by the thermal effects of the support bracket on the absorber tube.

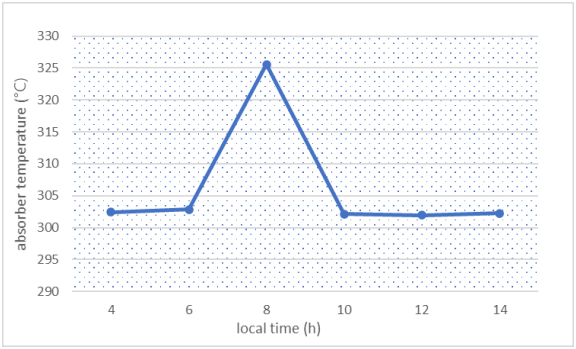

Figure 8: Daily comparison of the solar absorber output temperature of the proposed model to calculate the heat loss through the support bracket

According to Relations 6-11 and 6-12 and Figure 9, increasing the inlet temperature increases the convection heat transfer coefficient of HTF and decreases the thermal gain. On the other hand, the decrease in thermal gain leads to a decrease in the efficiency of the collector.

$$q\_gain = (h1 * D2 * pi * (T2(1) - T1 - 273.15)) * L$$

$$Efficiency = q\_gain/q\_ra0 * 100/L/W$$

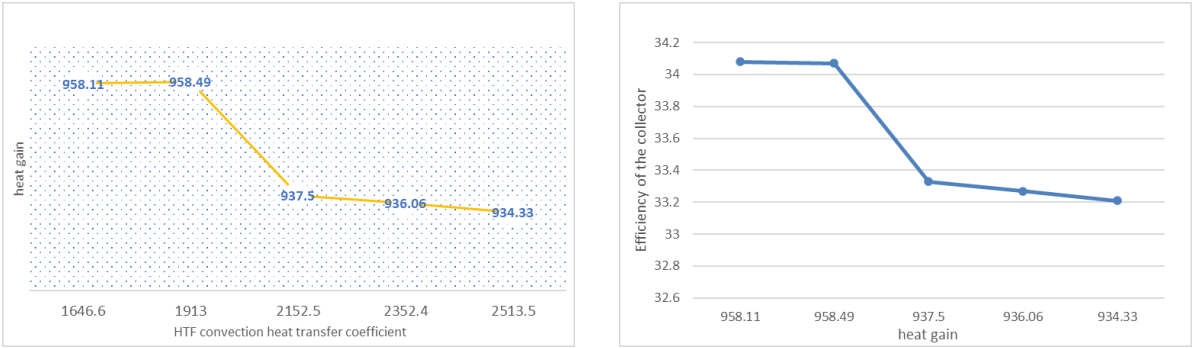

Figure 9: a) changes in thermal gain compared to HTF convection heat transfer coefficient, b) changes in collector efficiency compared to thermal gain

HTF flow rate is directly related to HTF fluid velocity. According to Equation 6-13 and Figure 10, the trend of mass flow rate is upward with increasing fluid speed.

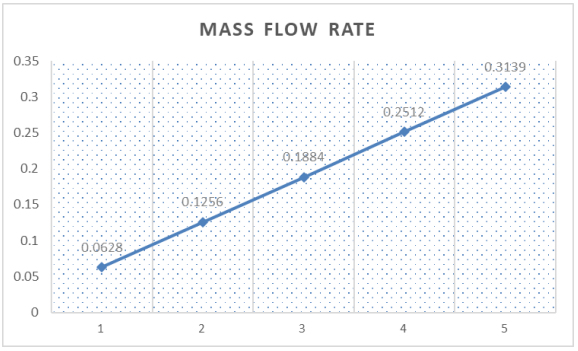

Figure 10: Changes of mass flow rate against fluid velocity

The numerical simulation results of the proposed PTSC mathematical models have been interpreted. The models developed in this study consider more physical phenomena and reflect the actual performance of a PTSC system, unlike the model of [29]. The difference between the results of [29] and the results of the proposed model is due to the quantitative and qualitative simplification of the significant negative effects of thermophysical phenomena governing the thermal behavior of the supporting brackets under the influence of solar radiation and ambient air. Padilla [23] has emphasized the effective thermal behavior of the support bracket in comparing his results with the results of [21]. Also, Kalogirou et al. [45, 46] attributed the observed discrepancy between the experimental and predicted values of the characteristic curve slope of a collector to the thermal losses of the support brackets and compared the advantages and disadvantages of this process.

Conclusion

With the aim of presenting a mathematical model of a PTSC in the climatic conditions of south and southeast Iran, this research is the first step of a longitudinal study on the concentration of solar technologies and their exploitation in the said territory. The main results of this study are stated as follows.

- This study provided the analysis conditions of the proposed model through thermal performance, fluid outlet temperature, and solar absorber. The thermal analysis performed shows that the support brackets are the source of heat loss in the system regarding quality and quantity. Recorded heat losses of one support bracket-based thermal model are different from another model.
- In general, the proposed model is sensitive to wind speed changes. This sensitivity is important when the wind speed varies between 2 m/s and 5 m/s. Beyond this range, the sensitivity gradually decreases. Therefore, not only optical aspects during abnormal direct radiation but also the contribution of the support bracket connected to the absorber tube as a source of heat loss in the system should be considered.

References

1. Hafner M, Tagliapietra S, Lucia de Strasser. Energy in Africa, Springer Briefs in Energy, chap 3, pages 47-72, 10.1007/978-3-319-92219-5_3.
2. Bernard BT, Chara-Dackou VS, Goron D, Babikir MH, Njomo D. Empirical relationships between global and diffuse radiation and sunshine duration in chad: polynomial regression approach. IJHT 2022;40(1):121–9. https://doi.org/ 10.18280/ijht.400114.
3. Chara-Dackou VS, Njomo D, Babikir MH, Mbouombouo IN, Pofoura Gboulie AS, Tchinda R. Processing Sunshine Duration Measurements for the Assessment of Solar Radiation in Climatic Regions of the Central African Republic, J Solar Energy Eng (2022) Vol. 144 1-15 (15 pages), 10.1115/1.4053483.
4. Babikir MH, Njomo D, Barka M, Khayal MY, Goron D, Chara-Dackou VS, et al. Modeling the incident solar radiation of the City of N'Djamena (Chad) by the Capderou method. Int J Photoenergy 2020;2020:6292147. https://doi.org/ 10.1155/2020/6292147.

5. Soulouknga MH, Doka SY, Revanna N, Djongyang N, Kofane TC. Analysis of wind speed data and wind energy potential in Faya-Largeau, Chad, using Weibull distribution. Renew Energy 2018;121:1–8. https://doi.org/10.1016/j. renene.2018.01.002.
6. Didane DH, Rosly N, Zulkafli MF, Shamsudin SS. Evaluation of wind energy potential as a power generation source in Chad. Int J Rotating Mach 2017;2017: 1–10. https://doi.org/10.1155/2017/3121875. Article ID 3121875.
7. Tiwari AK, Kalamkar VR. Effects of total head and solar radiation on the performance of solar water pumping system. Renew Energy 2018;118:919–27. https://doi.org/10.1016/j.renene.2017.11.004.
8. Errouha M, Derouich A, El Ouanjli N, Motahhir S. High-performance standalone photovoltaic water pumping system using induction motor. Int J Photoenergy 2020;2020:1–13. https://doi.org/10.1155/2020/3872529. Article ID 3872529.
9. Babikir MH, Chara-Dackou VS, Njomo D, Barka M, Khayal MY, Legue DRK, et al. Simplified modeling and simulation of electricity production from a dish/stirling system. Int J Photoenergy 2020;2020:1–14. https://doi.org/10.1155/2020/ 7398496. Article ID 7398496.
10. Fernandez-Garcıa A, Zarza E, Valenzuela L, Perez M. Parabolic-trough solar collectors and their applications. Renew Sustain Energy Rev 2010;14:1695–721. https://doi.org/10.1016/j.rser.2010.03.012.
11. Al-Sulaiman FA, Zubair MI, Atif M, Gandhidasan P, Al-Dini SA, Antar MA. Humidification dehumidification desalination system using parabolic trough solar air collector. Appl Therm Eng 2015;75:809e816. https://doi.org/10.1016/j. applthermaleng.2014.10.072.
12. Fathabadi H. Novel low-cost parabolic trough solar collector with TPCT heat pipe and solar tracker: performance and comparing with commercial flat-plate and evacuated tube solar collectors. Sol Energy 2020;195:210–22. https://doi.org/ 10.1016/j.solener.2019.11.057.
13. Ashouri M, Vandani AMK, Mehrpooya M, Ahmadi MH, Abdollahpour A. Technoeconomic assessment of a Kalina cycle driven by a parabolic Trough solar collector. Energy Convers Manage 2015;105:1328–39. https://doi.org/10.1016/j. enconman.2015.09.015. [14] Yılmaz IH, Mwesigye A. Modeling, simulation and performance analysis of parabolic trough solar collectors: a comprehensive review. Appl Energy 2018;225: 135–74. https://doi.org/10.1016/j.apenergy.2018.05.014.
14. Dudley V, Kolb G, Sloan M, Kearney D. SEGS LS2 Solar Collector-Test Results. Report of Sandia National Laboratories. SAN94-1884; 1994.
15. Bellos E, Tzivanidis C. Alternative designs of parabolic trough solar collectors. Prog Energy Combust Sci 2019;71:81–117. https://doi.org/10.1016/j. pecs.2018.11.001.
16. Huang W, Hub P, Chen Z. Performance simulation of a parabolic trough solar collector. Sol Energy 2012;86:746–55. https://doi.org/10.1016/j. solener.2011.11.018.
17. Wang Y, Liu O, Lei J, Jin H. A three-dimensional simulation of a parabolic trough solar collector system using molten salt as heat transfer fluid. Appl Therm Eng 2014;70:462e476. https://doi.org/10.1016/j.applthermaleng.2014.05.05.
18. Liang H, You S, Zhang H. Comparison of three optical models and analysis of geometric parameters for parabolic trough solar collectors. Energy 2016;96:37e47. https://doi.org/10.1016/j.energy.2015.12.050.
19. Balghouthi M, Ali ABH, Trabelsi SE, Guizani A. Optical and thermal evaluations of a medium temperature parabolic trough solar collector used in a cooling installation. Energy Convers Manage 2014;86:1134–46. https://doi.org/10.1016/j. enconman.2014.06.095.
20. Forristall R. Heat transfer analysis and modeling of a parabolic trough solar receiver implemented in engineering equation solver. National Renewable Energy Laboratory (NREL); 2003.
21. Ricardo VP, Gokmen D, Goswami DY, Stefanakos E, Muhammad MR. Heat transfer analysis of parabolic trough solar receiver. Appl Energy 2011;88:5097–110. https://doi.org/10.1016/j.apenergy.2011.07.012.
22. Ricardo VP. Simplified Methodology for Designing Parabolic Trough Solar Power Plants. University of South Florida; 2011.

23. Qin C, Kim JB, Lee BJ. Performance analysis of a direct-absorption parabolictrough solar collector using plasmonic nanofluides. Renewable Energy 2019;143: 24e33. https://doi.org/10.1016/j.renene.2019.04.146.
24. Olia H, Torabi M, Bahiraei M, Ahmadi MH, Goodarzi M, Safaei MR. Application of nanofluids in thermal performance enhancement of parabolic trough solar collector: state-of-the-art. Appl Sci 2019;9:463. https://doi.org/10.3390/ app9030463.
25. Krishna Y, Faizal M, Saidur R, Ng KC, Aslfattahi N. State-of-the-art heat transfer fluids for parabolic trough collector. Int J Heat Mass Transf 2020;152:119541. https://doi.org/10.1016/j.ijheatmasstransfer.2020.119541.
26. Marif Y, Benmoussa H, Bouguettaia H, Belhadj MM, Zerrouki M. Numerical simulation of solar parabolic trough collector performance in the Algeria Saharan region. Energy Convers Manage 2014;85:521–9. https://doi.org/10.1016/j. enconman.2014.06.002.
27. Marefati M, Mehrpooya M, Shafii MB. Optical and thermal analysis of a parabolic trough solar collector for production of thermal energy in different climates in Iran with comparison between the conventional nanofluides. J Clean Prod 2018;175 (20):294–313. https://doi.org/10.1016/j.jclepro.2017.12.080.
28. Babikir MH, Njomo D, Barka M, Chara-Dackou VS, Kondji YS, Khayal MY. Thermal modeling of a parabolic trough collector in a quasi-steady state regime. J Renewable Sustainable Energy 2021;13:013703. https://doi.org/10.1063/ 1.5145272.
29. Liang H, You S, Zhang H. Comparison of different heat transfer models for parabolic trough solar Collectors. Appl Energy 2015;148:105–14. https://doi.org/ 10.1016/j.apenergy.2015.03.059.
30. Delcea C, Siserman C. The emotional impact of COVID-19 on forensic staff. Rom J Leg Med. 2021 Mar 1;29(1):142-6.
31. Marif Y, Chiba Y, Belhadj MM, Zerrouki M, Benhammou M. A clear sky irradiation assessment using a modified Algerian solar atlas model in Adrar city. Energy Rep 2018;4:84–90. https://doi.org/10.1016/j.egyr.2017.09.002.
32. Arim AI, Babikir MH, Chara-Dackou VS, Njomo D. Modeling and simulation of hourly irradiance for solar applications in Chad: case of the city of Abeche. Int J Heat Technol 2022;40(4):976–86. https://doi.org/10.18280/ijht.400415.
33. Xu C, Chen Z, Li M, Zhang P, Ji X, Luo X, et al. Research on the compensation of the end loss effect for parabolic trough solar collectors. Appl Energy 2014;115(15): 128–39. https://doi.org/10.1016/j.apenergy.2013.11.003.
34. Hoseinzadeh H, Kasaeian A, Shafii MB. Geometric optimization of parabolic trough solar collector based on the local concentration ratio using the Monte Carlo method. Energy Convers Manage 2018;175:278–87. https://doi.org/10.1016/j. enconman.2018.09.001.
35. Alfellag MAA. Modeling and Experimental Investigation of Parabolic Trough Solar Collector, Doctoral Dissertations and Master's Theses (2014). 11, https://comm ons.erau.edu/edt/11.
36. Behar O, Khellaf A, Mohammedi K. A novel parabolic trough solar collector model – Validation with experimental data and comparison to Engineering Equation Solver (EES). Energy Convers Manage 2015;106:268–81. https://doi.org/10.1016/ j.enconman.2015.09.045.
37. Gaul H, Rabl A. Incidence-angle modifier and average optical efficiency of parabolic trough collectors. J Sol Energy Eng 1980;102(1):16–21. https://doi.org/ 10.1115/1.3266115.
38. Rabl A. Active solar collectors and their applications. USA: Oxford University Press; 1985.
39. Lippke F. Simulation of the part-load behavior of a 30 MWe SEGS plant. Technical report, SAND-95-1293. Albuquerque, NM, US: Sandia National Laboratories; 1995.
40. Kakat S, Shah RK, Aung W. Handbook of single-phase convective heat transfer. New York: John Wiley & Sons; 1987. [41] Gnielinski V. On heat transfer in tubes. Int J Heat Mass Transf 2013;63:134–40. https://doi.org/10.1016/j.ijheatmasstransfer.2013.04.015.
41. Cavalu S, Simon V, Albon C, Hozan C. Bioactivity evaluation of new silver doped bone cement for prosthetic surgery. J Optoelectron Adv Mater. 2007 Mar 1;9(3):690.

42. Delcea C, Rad D, Gyorgy M, Runcan R, Breaz A, Gavrilă-Ardelean M, Bululoi AS. A network analysis approach to Romanian resilience-coping mechanisms in the Covid-19 era. Pharmacophore. 2023;14(4-2023):57-63.
43. Galea-Holhoș LB, Delcea C, Siserman CV, Ciocan V. Age estimation of human remains using the dental system: A review. Ann Dent Spec. 2023;11(3-2023):14-8.
44. Hoffmann JF, Vaitilingom G, Henry JF, Chirtoc M, Olives R, Goetz V, et al. Temperature dependence of thermophysical and rheological properties of seven vegetable oils in view of their use as heat transfer fluids in concentrated solar plants. Sol Energy Mater Sol Cells 2018;178:129–38. https://doi.org/10.1016/j. solmat.2017.12.037.
45. Kalogirou SA, Lloyd S, Ward J, Eleftheriou. Design and performance characteristics of a parabolic-trough solar-collector system. Appl Energy 1994;47 (4):341–54. https://doi.org/10.1016/0306-2619(94)90041-8.
46. Kalogirou SA. A detailed thermal model of a parabolic trough collector receiver. Energy 2012;48(1):298–306. https://doi.org/10.1016/j.energy.2012.06.023.